

Contrasting Fates of Petrogenic and Biospheric Carbon in the South China Sea

Journal Article**Author(s):**

Blattmann, Thomas M.; Zhang, Y.; Zhao, Y.; Wen, K.; Lin, S.; Li, J.; Wacker, Lukas; Haghypour, Negar; Plötze, Michael; Liu, Z.; Eglinton, Timothy I.

Publication date:

2018-09-16

Permanent link:

<https://doi.org/10.3929/ethz-b-000302172>

Rights / license:

[Creative Commons Attribution-NonCommercial-NoDerivatives 4.0 International](#)

Originally published in:

Geophysical Research Letters 45(17), <https://doi.org/10.1029/2018GL079222>

RESEARCH LETTER

10.1029/2018GL079222

Key Points:

- Marine and petrogenic OC dominantly contribute to bulk POC in abyssal sediments
- Soil OC is absent in deep-sea sediments due to preferential loss and deposition on proximal shelf
- Al-¹⁴C trend indicates loss of soil OC from lithogenic particles with lowest ¹⁴C values thus far reported for deep ocean POC

Supporting Information:

- Supporting Information S1
- Data Set S1

Correspondence to:

T. M. Blattmann and Y. Zhang,
thomas.blattmann@erdw.ethz.ch;
ywzhang@tongji.edu.cn

Citation:

Blattmann, T. M., Zhang, Y., Zhao, Y., Wen, K., Lin, S., Li, J., et al. (2018). Contrasting fates of petrogenic and biospheric carbon in the South China Sea. *Geophysical Research Letters*, 45, 9077–9086. <https://doi.org/10.1029/2018GL079222>

Received 15 JUN 2018

Accepted 8 AUG 2018

Accepted article online 14 AUG 2018

Published online 6 SEP 2018

©2018. The Authors.

This is an open access article under the terms of the Creative Commons Attribution-NonCommercial-NoDerivs License, which permits use and distribution in any medium, provided the original work is properly cited, the use is non-commercial and no modifications or adaptations are made.

Contrasting Fates of Petrogenic and Biospheric Carbon in the South China Sea

T. M. Blattmann¹ , Y. Zhang² , Y. Zhao², K. Wen², S. Lin², J. Li², L. Wacker³ , N. Haghipour¹ , M. Plötze⁴ , and T. I. Eglinton¹ 

¹Geological Institute, ETH Zurich, Zurich, Switzerland, ²State Key Laboratory of Marine Geology, Tongji University, Shanghai, China, ³Laboratory of Ion Beam Physics, ETH Zurich, Zurich, Switzerland, ⁴Institute for Geotechnical Engineering, ETH Zurich, Zurich, Switzerland

Abstract A synthesis of published and newly acquired stable and radiocarbon isotope data from soil, river, and marine particulate organic carbon (OC) from the South China Sea drainage and sedimentary basin reveals that OC derived from bedrock-erosion (petrogenic OC) and marine productivity comprises the major contributors to bulk OC in particulate matter reaching abyssal depths, while soil-derived OC appears negligible. Aluminum-radiocarbon relationships of sediments suggest that soil OC initially associated with detrital terrestrial minerals is lost and replaced by marine OC during transport beyond the continental shelf. We estimate that petrogenic OC sinking to a ~30,000 km² region of the deep northeastern South China Sea accounts for 0.6% of global petrogenic OC burial. The basin-wide OC isotope patterns coupled with sediment trap observations highlight both the spatial variabilities of OC components as they propagate from source to sedimentary sink and the significance of petrogenic OC to deep ocean sediments.

Plain Language Summary Sediment traps deployed in the ocean intercept settling particulate organic matter of marine and terrestrial origin. Terrestrial organic matter includes contributions from soils as well as bedrock-derived organic matter mobilized by erosional processes and is exported by rivers into the ocean, where it contributes to sinking sediment fluxes. In this sediment trap study from the northeastern South China Sea, we constrain the flux and type of organic carbon exported to the deep ocean using stable and radiocarbon isotopes. We find that bedrock-derived and marine organic matter comprise the dominant types of sedimentary organic matter reaching the deep South China Sea, whereas soil organic matter is conspicuously absent. Both bedrock-derived carbon and marine carbon are associated with terrestrial mineral particles as revealed by the high aluminum contents of all collected sediments, implying that soil organic matter must be lost from mineral surfaces and replaced with marine carbon. These findings raise fundamental new questions concerning the role of organic matter-mineral interactions in the ocean.

1. Introduction

Over 99% of reduced organic carbon (OC) on Earth is found as *kerogen* disseminated in ancient sedimentary rocks, with this vast carbon pool affecting biogeochemical cycles on geological timescales (Hedges, 1992). As rock-derived or *petrogenic* organic carbon (OC_{petro}) is exposed at the Earth's surface and eroded, its intrinsic recalcitrance—having survived diagenetic and metamorphic processes associated with burial, lithification, and exhumation—implies that it may exhibit conservative behavior, largely bypassing the *complicated* carbon cycle first recognized by Matti Sauramo (1938, 1939) during subsequent mobilization and transport. The balance between oxidation and reburial of OC_{petro} modulates the oxygen and carbon dioxide content of the atmosphere over geological timescales (Bernier, 1990; Hedges, 1992). OC contents of sediments reflect recent organic matter (OM) production derived from terrestrial and aquatic biospheres (OC_{bio}) intermixed with OC_{petro} from physical erosion of bedrock (Galy et al., 2015). Carbon isotopic mixing models assist in disentangling the contributions from these respective components and provide quantitative constraints on OC_{petro} versus OC_{bio} contents necessary to disentangle OC sources (e.g., Hilton et al., 2015).

From the context of sediment provenance, the South China Sea (SCS) is arguably one of the best constrained marginal sea systems in the world due to the pronounced gradients in clay mineralogical assemblage associated with its different source regions (Liu, Colin, et al., 2010; Liu et al., 2016). Taiwan has been recognized as an important source of OC_{petro} to the northeast SCS (Zheng et al., 2017), with the occurrence of OC_{petro} in modern Taiwanese rivers first reported by Kao and Liu (1996), and the efficiency of OC_{petro} export to the

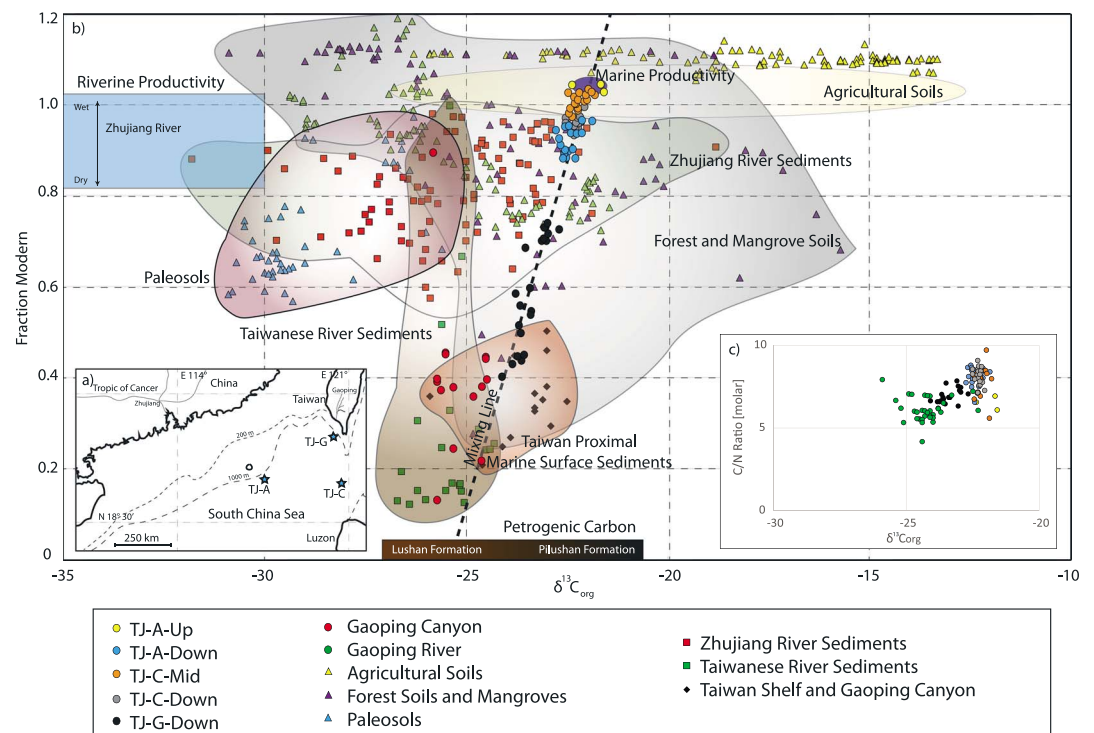


Figure 1. (a) Map of mooring stations TJ-A, TJ-C, and TJ-G. (b) Fm and $\delta^{13}C$ catchment-wide overview of the South China Sea comprising soil, river, marine surface sediments, and sediment trap data. Soils are categorized into agricultural soils, forest and mangrove soils, and paleosols. The agricultural soils include profiles from Taiwan and Luzon (Becker-Heidmann et al., 1996). The forest (Ding et al., 2010; Shen, Sun, et al., 2001; Shen, Yi, et al., 2001; Shen et al., 2004) and mangrove (Zhang et al., 2012; Zhang et al., 2013) soil profiles and paleosols (Ding et al., 2012) all come from mainland China. Fluvial sediments include Zhujiang River (Gao et al., 2007; Liu et al., 2017; Tao et al., 2012; Wei, Shen, et al., 2010; Wei, Yi, et al., 2010) and southwestern Taiwanese rivers (Kao et al., 2014). Radiocarbon isotopic composition of Zhujiang River dissolved inorganic carbon given by Liu et al. (2017). Marine surface sediments are from the Gaoping Canyon and adjacent shelf (Kao et al., 2014). Sediment trap samples proximal to Taiwan (Kao et al., 2014; Zheng et al., 2017) and in the deep South China Sea are highlighted in the figure. Characteristic source end member carbon isotopic compositions are outlined. (c) C/N ratio versus $\delta^{13}C$ of bulk organic matter with data from Gaoping River reported by Hilton et al. (2010).

ocean from this orogen highlighted by Hilton et al. (2011). Globally, it has been estimated that 43_{-25}^{+61} Mt OC_{petro} are discharged from land to ocean annually (Galy et al., 2015). Taiwan discharges a disproportionately high amount of OC_{petro} , comprising 3% of this global annual land-ocean flux (Wang et al., 2016). Sediments discharged from the Gaoping River draining southwestern Taiwan largely bypass the narrow shelf and slope environments, where very little terrestrial sediment is trapped, and a large fraction is exported directly into the deep ocean (Hsu et al., 2014; Kao et al., 2014; Zhang et al., 2018). Here we examine the fate of both OC_{bio} and OC_{petro} in deep waters of the northern SCS in the context of Taiwan and adjacent continental inputs and investigate its relationship with lithogenic sedimentary particles.

2. Materials and Methods

Bottom-tethered sediment trap moorings detailed in Zhang et al. (2014; 2018) were deployed in May 2014 and recovered in May 2015 at three stations, TJ-A, TJ-C, and TJ-G with local water depths of $\sim 2,100$, $\sim 3,850$, and $\sim 2,100$ m, respectively (Figure 1a). At these three mooring sites, five sediment traps are subject of this investigation including: TJ-A-Up (~ 510 m), TJ-A-Down ($\sim 1,960$ m), TJ-C-Mid ($\sim 2,045$ m), TJ-C-Down ($\sim 3,795$ m), and TJ-G-Down ($\sim 2,055$ m). Each sediment trap consists of 21 sampling bottles of 500 ml, filled with seawater containing $HgCl_2$ and NaCl, continuously collecting settling particles for a whole year at 18-day time intervals. Upon recovery, sediment trap samples were kept cool at 4 °C until they were sieved (<1 mm), split, washed by filtration, and oven-dried at 40 °C for ≥ 48 hr in the State Key Laboratory of

Marine Geology at Tongji University, Shanghai. Aluminum contents were measured by inductively coupled plasma-optical emission spectroscopy (ICP-OES) following methods and sample pretreatment established at Tongji University, Shanghai (Liu et al., 2009). The total OC and nitrogen content as well as radiocarbon and stable carbon isotope composition of bulk OC were measured on an elemental analyzer-isotope ratio mass spectrometer (EA-IRMS, Elementar vario MICRO cube—Isoprime visION) coupled to a Mini Carbon Dating System (MICADAS) accelerator mass spectrometer at ETH Zurich (Ionplus; McIntyre et al., 2016). Inorganic carbon was removed prior to measurement using an in-cup hydrochloric acid vapor fumigation method at 65 °C for three days (Hedges & Stern, 1984; Komada et al., 2008). All contents, including nitrogen, were measured on acidified sample material. Analytical reproducibility of stable carbon isotopic composition is reported as one standard deviation based on reproducibility of in-house atropine standard run in parallel to samples. Radiocarbon isotopic data were reduced using BATS software (Wacker et al., 2010) and corrected for constant extraneous carbon contamination (Wacker & Christl, 2011; Table S1 for data and propagated errors). Dissolved inorganic carbon was collected from ocean surface waters at all mooring locations following procedures described in Blattmann et al. (2018). These were analyzed for their radiocarbon isotopic composition by sparging the CO₂ into the gas ion source of the MICADAS AMS (Wacker et al., 2013).

3. Results and Discussion

3.1. Carbon Isotope End Members in the SCS

Characteristic source end member carbon isotopic compositions are comprehensively outlined by synthesizing catchment-wide relevant sediments surrounding the SCS (Figure 1b). In the context of these source regions, carbon isotope data for all sediment trap data available from the SCS are highlighted. The terrestrial OC sources include soils and river sediments from South China, Taiwan, and Luzon. The carbon isotopic characteristics of OC sourced from soils and rivers exhibit a large spread in stable carbon isotope (exceeding the range of -15 to -30‰) and radiocarbon isotope (from bomb to near ^{14}C -dead) composition reflecting OC type (freshwater aquatic, C3, and C4) and OC age as related to soil OC turnover, reservoir effects, and contributions of OC_{petro}. These carbon isotope end members are discussed in Texts S1 and S2.

The $\delta^{13}\text{C}$ and C/N ratio values are typically used to identify sedimentary OM sources with marine and terrestrial OC in the SCS characterized by values of $-22.1 \pm 1.1\text{‰}$, C/N 6.63 ± 1 , and -25.5‰ , C/N 22, respectively (Liu et al., 2007; Meyers, 1994). In the SCS (Figure 1c), terrestrial input from the Gaoping River is characterized by relatively low C/N molar ratios (~ 6) and $\delta^{13}\text{C}$ values (mostly between -25 and -24‰), reflecting high contributions of bedrock-derived OM (Hilton et al., 2010). Traps TJ-G-Down, TJ-A-Down, TJ-C-Down, and TJ-C-Mid are characterized by higher $\delta^{13}\text{C}$ values and C/N ratios, approaching -22‰ and 8, respectively. The measured ^{14}C contents of bulk OC from sediment trap TJ-G-Down represent the lowest ever reported for deep-sea sediment traps ($\geq 2,000$ m) globally. Given these very ^{14}C -depleted signatures within the Gaoping Submarine Canyon, it is evident that OC_{petro} must be a major contributor to OC supplied to deep-sea basin.

3.2. Organic Carbon Provenance in the Deep SCS

The ^{13}C versus ^{14}C ($\delta^{13}\text{C}$ vs Fm) plot shown in Figure 1b reveals that all of the deep SCS sediment trap samples from the 2014–2015 deployment lie on a line ($R^2 = 0.89$). This suggests that sinking particulate OC (POC) contains varying proportions of OC derived chiefly from only two sources, with one component evidently being OC_{petro} sourced from Taiwan. The second source is assigned to marine productivity, because (i) TJ-A-Up (~ 510 -m water depth), which is most influenced by upper ocean (biological pump) processes and is most distal from land, exhibits stable carbon isotopic characteristics consistent with this end member; (ii) contributions of soil OC should introduce more scatter into the data due to their more varied carbon isotopic compositions as a function of depth and soil type; and (iii) radiocarbon contents decrease with increasing total sediment flux (Figure S1), coherent with lateral influx of OC_{petro} diluting marine input. The marine OC mirrors the radiocarbon content of the ocean surface water dissolved inorganic carbon, which averages 1.04 ± 0.01 Fm ($n = 7$). Additionally, the $\delta^{13}\text{C}$ signatures of the marine ($-22.0 \pm 0.1\text{‰}$) and petrogenic ($-25.4 \pm 0.1\text{‰}$) OC end members, defined by Fm values of 1.04 and 0 for the linear regression in Figure 1b, respectively, are identical to the marine ($-22.1 \pm 1.1\text{‰}$) and *terrigenous* (-25.5‰) end members adopted in previous time series surveys of water column suspended sediments from the photic zone and deep waters in the SCS (Liu et al., 2007). These results indicate an absence of

inputs of isotopically-heavy terrigenous OC that would otherwise overlap with the marine end member, despite the presence of such isotopic pedogenic OC signatures on land. Thus, from a bulk compositional perspective, soil OC contributions to deep-ocean sinking POC appear to be negligible, and consequently, sedimentation of terrigenous OC in the northern SCS is overwhelmingly dominated by petrogenic OC. This sharp contrast in fate of petrogenic and pedogenic OC implies that the latter is either remineralized or preferentially deposited in more land-proximal shelf or slope environments. This export of OC_{petro} to the deep SCS reveals strong sorting of sedimentary OC and supports the notion that fresh pedogenic OC is trapped on the continental margin (Zheng et al., 2017), potentially in muddy regimes along submarine canyon flanks, where high terrestrial OC-burial fluxes have been previously described (Hsu et al., 2014).

The northeastern SCS primarily receives terrestrial sediment from sources with the following sediment fluxes: (1) Taiwan 176 Mt/year, (2) South China 102 Mt/year, and (3) Luzon >13 Mt/year (Liu et al., 2016). The deep northeastern SCS is characterized by clay mineral assemblages composed mainly of illite, chlorite, and smectite, while sediments with abundant kaolinite proportions, characteristic of the Zhujiang River, are restricted to shelf environments hugging the Chinese mainland (Liu et al., 2016; Liu, Colin, et al., 2010). It thus appears that soil OM sourced from the Zhujiang River, which evades remineralization, may find a fate similar to that of kaolinite, with which it is likely associated, leading to its deposition on the wide shelf (>200 km) separating the Chinese mainland from the deep SCS. The absence of a soil OC signature in the deep SCS suggests that despite the Zhujiang River being one of the world's largest rivers by discharge, its ultimate legacy in terms of the deep SCS sediment record is disproportionately small, at least during interglacial periods. In contrast, the shelf areas around Taiwan and Luzon facing the northeastern SCS are very narrow, allowing terrestrial sediments to reach the deep northeastern SCS (as shown by clay mineral composition of marine surface sediments; Liu et al., 2016). Nevertheless, despite this limited accommodation space, biomolecular analysis of turbidity current-entrained sediments sourced from Taiwan, collected within the triangle spanned by the moorings of this study at bathypelagic depths in the wake of historic Typhoon Morakot in 2008, revealed that fatty acids, an abundant lipid class (800–1,000 $\mu\text{g/g}$), were predominantly of marine origin, whereas less-abundant sterol signatures (10–20 $\mu\text{g/g}$) suggested mixed terrestrial and marine contributions (Selvaraj et al., 2015). Thus, only vestigial molecular remains of pedogenic OC apparently persist in the bathypelagic realm of the SCS despite entrainment of terrestrially derived sediments in turbidity currents, consistent with the inferred predominance of OC_{petro} based on the isotopic composition of bulk OC in settling particles intercepted by the sediment traps. Furthermore, challenging previous conjectures that suggested indiscriminate transfer of all types of terrestrial OC by turbidity currents (Kao et al., 2014; Liu et al., 2012; Zheng et al., 2017), we find that the increased export efficiency of terrestrial OC into the bathypelagic realm is highly selective toward OC_{petro} .

The stable carbon isotopic composition of the OC_{petro} end member ($F_m = 0$ by definition) was centered at -25.4‰ during the 2014–2015 sediment trap campaign. Given the strong erosion, exposing bedrock in the wake of extreme weather events (Tsai et al., 2010), this isotopic fingerprint can conceivably vary with time. At this stage, caution should be exercised in interpreting potential shifts through time as differences in sample preparation, measurement, and data correction may introduce offsets between the data sets reported previously (Kao et al., 2014; Zheng et al., 2017) and this study. However, assuming that the data sets are comparable, $\delta^{13}\text{C}_{OC_{\text{petro}}}$ appears to exhibit a lower value in 2008 (Kao et al., 2014; Zheng et al., 2017). This change in OC_{petro} signature from the southwestern Taiwan catchment over timescales of years may reflect differential erosion of OC_{petro} from different formations. Within the mountainous region of the Gaoping River catchment, the two formations comprising the vast majority of areal bedrock exposure are the (1) Lushan Formation (approximately two thirds of the mountainous catchment area, $\delta^{13}\text{C}_{\text{org}} = -25.3 \pm 1.7\text{‰}$, $n = 5$) and (2) Pilushan Formation (approximately one fourth of the mountainous catchment area, $\delta^{13}\text{C}_{\text{org}} = -22.4 \pm 1.5\text{‰}$, $n = 5$; Hilton et al., 2010). Small areal contributions of low-grade sedimentary rocks from the foreland from the Cholan and Tuokoshan Formations are typically lighter (average $\delta^{13}\text{C}_{\text{org}} = -27.1\text{‰}$; Sparkes et al., 2015). From the calculated $\delta^{13}\text{C}$ of OC_{petro} in the traps and direct measurements on the rocks, it is apparent that the deep SCS is receiving OC_{petro} sourced predominantly from the Lushan Formation, which appears to compete with the isotopically heavier Pilushan Formation. More data from bedrock samples and from longer-term sediment trap time series using consistent methods are needed for in-depth comparison to test this hypothesis.

Previous studies have estimated fluvial OC_{petro} export (Kao et al., 2014) as well as net CO_2 sequestration from chemical weathering on Taiwan based on OC_{petro} oxidation and OC_{bio} burial (Hilton et al., 2014). As the journey of OC_{petro} does not end once it is discharged into the ocean, it is important to constrain the abyssal OC_{petro} fluxes in order to quantify the net effect on atmospheric CO_2 . Kao et al. (2014) argued in favor of conservative OC_{petro} transfer into the deep SCS, citing low dissolved oxygen contents and high accumulation rates. Although degradation of OC_{petro} within river basins during sediment transport has been studied (e.g., Bouchez et al., 2010), no such insights currently exist for the marine realm to support this assumption. OC in marine surface sediments collected from the shelf and land-proximal regions of the Gaoping Canyon ("Taiwan Proximal Marine Surface Sediments" in Figure 1, shaded in red) exhibits highly depleted radiocarbon contents, in line with substantial Taiwanese supply of OC_{petro} to the ocean. With respect to stable carbon isotopic compositions, these marine sediments show $\delta^{13}C_{\text{org}}$ values, which are both considerably lighter and heavier than that of the mixing line proposed for the 2014–2015 sediment trap samples. This suggests that pedogenic OC of either C_4 or C_3 origin or OC_{petro} sourced from different formations results in signature offsets from the mixing line. If marine OC strongly dilutes the terrestrial OC supply, pedogenic OC signatures may only become apparent once labile marine OC is remineralized upon final burial. Taiwanese OC_{petro} , having undergone higher grade metamorphism and thus exhibiting higher $\delta^{13}C_{\text{org}}$ values (Yui, 2005), may be more recalcitrant and undergo selective preservation during the final stages of transport and early diagenesis in surficial sediments. Revisions of previously estimated carbon budgets for weathering of mountain belts (Hilton et al., 2014) would be necessary if a significant fraction of OC_{petro} in the marine realm is indeed remineralized prior to burial. Remineralization of OC_{petro} has been observed within the Amazon River system (Bouchez et al., 2010), and it is thus likely that similar degradation may occur in the marine realm. Previous studies have used a $OC \times F_m$ versus OC crossplot for estimating average OC_{petro} content in sediments (Galy et al., 2008; Zheng et al., 2017). Applying this approach to the sediment trap data collected in this study (Figure S2) results in an average OC_{petro} of $0.37 \pm 0.08\%$, which has a higher tendency than nontyphoon sediment trap sediments within the upper Gaoping Canyon ($0.28 \pm 0.06\%$; Zheng et al., 2017), hinting that hydrodynamic sorting processes may result in preferential export of particles laden with OC_{petro} to the deep sea.

Here we develop an independent assessment of the annual OC_{petro} vertical flux into the deep SCS sediments based on our novel sediment trap-based observations of ocean bottom fluxes. The locations of the three mooring systems TJ-A, TJ-C, and TJ-G span a triangle with an areal coverage of nearly 30,000 km², comprising approximately one 25th of the deep SCS seafloor with water depth $\geq 2,000$ m, defining the area for the abyssal OC_{petro} flux estimate. Based on the annual average vertical OC_{petro} fluxes measured for the three corners of the triangle, we apply a bilinear model describing OC_{petro} in all points within the triangle and integrate over the entire area in order to yield a total annual OC_{petro} flux (Text S3). This is a highly simplified model for assessing flux over an enormous area that ignores effects of hydrodynamics, currents, and conduits of preferential transport such as the Manila Trench (Talling et al., 2013), along-slope transport driven by bottom flow (Liu et al., 2016) or focused accumulation of pelagic sediment on drift deposits (Kienast et al., 2005; Shipboard Scientific Party, 2000). In the current study, sediment trap TJ-G-Down is deployed on the levee of the Gaoping Submarine Canyon and includes time intervals with sediments sourced from turbidity currents (Zhang et al., 2018). We propose that a reasonable first-order estimate for pelagic OC_{petro} burial can be obtained using this approach. As sediment fluxes from trap studies are inherently biased with respect to fluxes from the bottom nepheloid layer below the trap and preferential transport along the thalweg of the canyon, this vertical flux estimate is considered conservative. Within the defined area, and for this deployment year, we estimate that 0.242 Mt OC_{petro} was exported to the underlying deep-sea sediments. Relative to estimates of total Taiwanese (Wang et al., 2016) and global OC_{petro} (Galy et al., 2015) export, this corresponds to an estimated sink of 19 and 0.6% of annual OC_{petro} export flux, respectively. This first-order estimate only takes vertical flux (intercepted by the bottom sediment trap) into account and is likely highly dependent on the year. Future consideration of lateral fluxes and geographic expansion to take into account deposition beyond the defined area is necessary to develop a full budget of OC_{petro} in the deep SCS.

3.3. Aluminum-¹⁴C Relationships in Global Context

The downward trend in radiocarbon contents with increasing aluminum content, obtained from oceanic settling particulate matter intercepted by sediment traps, has been attributed to resuspension of lithogenic sediment-associated OC (Figure 2; Hwang et al., 2008; Hwang et al., 2010). Although trends in Al-¹⁴C

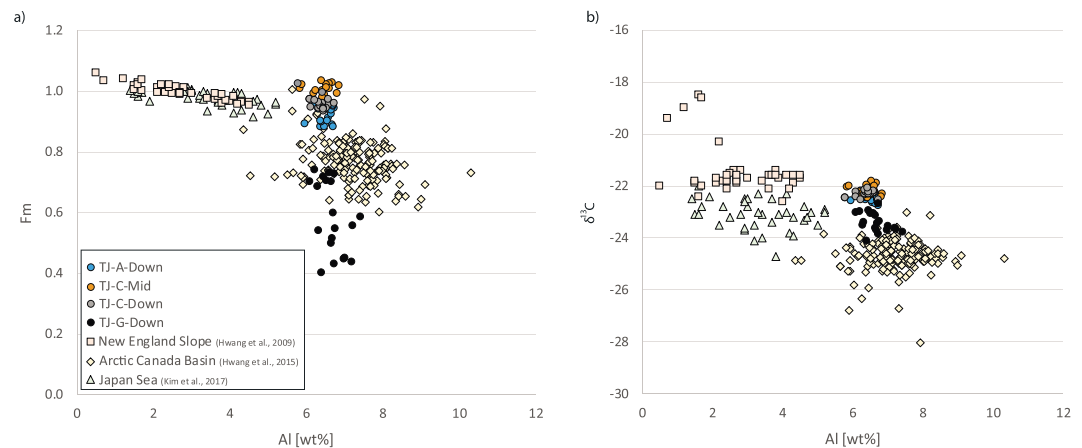


Figure 2. (a) Radiocarbon isotopic composition of bulk organic carbon versus aluminum content of sediment. (b) Stable carbon isotopic composition of bulk organic carbon versus aluminum content of sediment. The Japan Sea and New England Slope show mixing between a marine source ($F_m = 1$ and 0% Al content) with lithogenic material bearing an aged radiocarbon signature. The Arctic Canada Basin shows a more chaotic Al- ^{14}C - ^{13}C relationship characterized by relatively high aluminum contents throughout. The scatter and aged signature suggests contributions from aged terrestrial organic carbon and reworked marine sediments. In stark contrast, the SCS shows uniformly high Al contents but marked variations in ^{14}C and a subtle trend with ^{13}C , suggesting mixing between two predominantly lithogenic sources with one bearing a petrogenic carbon signature and the other a modern, marine signature.

relationships may be due to sediment resuspension, direct input of aluminosilicate-rich and aged OC-containing particulate matter constitutes an equally valid explanation. In the SCS, the decrease in radiocarbon content with a corresponding increase in aluminum content indicates binary mixing with the slope of the relationship clearly implying mixing between two sources supplying lithogenic material with vastly different radiocarbon isotopic compositions—one being modern and the other strongly depleted in ^{14}C . From the ^{14}C -depleted character of the TJ-G trap and from previous studies (Kao et al., 2014; Zheng et al., 2017), it is evident that OC_{petro} supplied by Taiwan is responsible for this contribution. As the decrease in lithogenic fraction in the distal traps is modest and given the primary presence together with marine OC, it is evident that any soil OC initially associated with the sedimentary aluminosilicates must have been lost, replaced, and diluted with marine OC to such an extent that its presence is no longer evident in bulk OC isotopic signatures. The active margins of Luzon and Taiwan stand in strong contrast the passive margin settings of the Canada Basin and New England Slope, where the ^{14}C -Al relationship was first observed. In particular, prior reports and in situ observations of frequent turbidity currents, which commonly originate from the Gaoping Submarine Canyon, promote efficient sediment and OC transfer to the deep sea adjacent to Taiwan (Dadson et al., 2005; Hilton et al., 2011; Hsu et al., 2014; Zhang et al., 2018), likely contributing to the pronounced ^{14}C -Al patterns observed in this study. It has been argued previously that active and passive margin settings differ greatly in their OC export and preservation patterns (Blair & Aller, 2012). Our observations also suggest that despite rapid export to the deep sea, soil OC may be lost very quickly. Similar to ^{14}C , ^{13}C -Al relationships in the SCS sinking particles also reflect increased contributions of (isotopically lighter) terrestrial OC with increased aluminum contents, supporting the notion that OC_{petro} contributions are diluted with marine OC. If fluvial sediments were deposited on the shelf environments and subject to reworking, we would expect a continuous degradation of terrestrial OC and addition of marine OC, leading to a weakening of the ^{14}C - and ^{13}C -Al trends. While controls on the carbon isotope-aluminum relationships remain speculative, it is evident from the SCS observations that OC_{petro} remains associated with and is closely coupled to sedimentation of lithogenic minerals. In addition, while clay minerals of pedogenic origin are also strongly represented in addition to bedrock-derived aluminosilicates and contribute to the lithogenic mineral fraction (Liu et al., 2016), pedogenic OC appears to lose this association, with indiscernible vestiges of this environmental bulk carbon isotope signature manifesting itself in settling sediments in the deep SCS.

3.4. Implications

Differential across-shelf export and preferential preservation of OC_{petro} in deep SCS sediments imply that the terrestrial signature recorded in bulk OC may be primarily of petrogenic origin. It is thus expected that deep-

sea surface sediments retrieved from settings beyond the continental margin in the SCS record terrestrial organic geochemical signatures related primarily to the erosion of bedrock. Proxies such as bulk OC isotopes and even biomarkers such as alkanes, which may be of petrogenic origin, should therefore be interpreted with caution given that they may partially reflect bedrock signatures in addition to commonly extracted information about continental vegetation (Zhou et al., 2017) and atmospheric CO₂ content (Kienast et al., 2001). The negligible input of terrestrial biospheric OC in the modern SCS may contrast sharply to glacial periods when lower sea level permitted greater terrigenous export into the OC into the deep SCS (Zhao et al., 2017). For example, increases in kaolinite contributions during the most recent glacial period mark heightened contributions from the Chinese mainland (Liu, Li, et al., 2010) that likely coincide with elevated pedogenic OC contributions, which evaded trapping on the shelf and margin areas. Nevertheless, it is evident that terrestrial OC in deep-sea sediments, even within the tropics, may be predominantly petrogenic in origin. It is within the terrestrial OC export hot spot of Southeast Asia (Schlünz & Schneider, 2000) that Taiwan and likely other source terrains characterized by short, steep river catchments (Komada et al., 2004) in this region deliver vast amounts of OC_{petro} to the ocean. However, in contrast to biospheric OC, the remineralization of OC_{petro} results in the net release of carbon dioxide to the atmosphere, while its burial has no net effect on atmospheric chemistry (Galy et al., 2008; Hedges, 1992). The observations from this study are consistent with limited remineralization and high efficiency export of OC_{petro} into the deep sea. Incorporation of OC_{petro} fluxes into biogeochemical and atmospheric models are needed to assess the effects of active orogens like Taiwan and other potential OC_{petro} sources in Southeast Asia on atmospheric chemistry.

The observed aluminum-carbon isotope relationships in settling particles from the SCS clearly indicate that terrigenous minerals, which initially must have been associated with some form of terrestrial OC, are repopulated with OC of marine origin in the deep ocean. Given the abundance of pedogenic sedimentary aluminosilicate particles found in the SCS catchment (Liu et al., 2009; Liu et al., 2016), pedogenic OC associated with such mineral phases appears to be lost beyond the margin environment. In contrast, OC_{petro} exhibits a more enduring affinity to aluminosilicates such as bedrock-derived illite and chlorite (Liu et al., 2016; Wang et al., 2016), possibly due to its encapsulation within shale-derived lithoclasts, which act as high-density agents of transport and protection. These observations imply that OC-aluminosilicate relationships are more dynamic than generally considered, challenging existing paradigms concerning (controls on) OC preservation in deep-sea sediments. Globally, the terrestrial OC component in deep-sea records inherits a distorted preservation pattern with the petrogenic signature dominating.

4. Conclusions

Petrogenic OC sourced from Taiwan mixes with marine OC as it is transported to and dispersed within the deep SCS. In contrast to the efficient transfer of petrogenic OC to the deep SCS, there is little evidence for export and sequestration of terrestrial biospheric OC from surrounding catchments (South China, Taiwan, and Luzon) in the SCS deep basin. Aluminum-radiocarbon relationships suggest that either terrestrial OC associated with mineral soils is preferentially deposited in land-proximal regions or that it undergoes loss from lithogenic mineral surfaces and replacement by marine OC during transport and sedimentation. Overall, in the context of carbon isotope characteristics of terrestrial source regions of the SCS, we find that only a very specific terrestrial component, OC_{petro}, ultimately dictates deep ocean terrestrial POC flux. In a first estimate of OC_{petro} flux over an expansive swath of ocean floor based on direct sediment trap observations, we calculate an annual deposition flux of 0.242 Mt OC_{petro} over a 30,000 km² swath of the deep northeastern SCS, accounting for approximately 19% of total OC_{petro} exported from Taiwanese rivers and 0.6% globally. Future assessments of OC_{petro} directly into the seafloor will help constrain the global carbon cycling and ultimate preservation efficiency of OC_{petro} during its source-to-sink transport.

References

- Becker-Heidmann, P., Scharpenseel, H.-W., & Wiechmann, H. (1996). Hamburg radiocarbon thin layer soils database. *Radiocarbon*, 38(02), 295–345. <https://doi.org/10.1017/S0033822200017665>
- Berner, R. A. (1990). Atmospheric carbon dioxide levels over Phanerozoic time. *Science*, 249(4975), 1382–1386. <https://doi.org/10.1126/science.249.4975.1382>
- Blair, N. E., & Aller, R. C. (2012). The fate of terrestrial organic carbon in the marine environment. *Annual Review of Marine Science*, 4(1), 401–423. <https://doi.org/10.1146/annurev-marine-120709-142717>

Acknowledgments

We thank Daniel Montluçon and Yanli Li for technical and laboratory assistance. We thank Meng Wang, Pingyuan Li, Shaohua Zhao, Ronan Joussain, Xuan Lyu, Shiwen Zhou, and Neil K. S. Cheong for their hard work during the cruises. The crew of the R/V Tianying is thanked for their fieldwork support. This manuscript benefitted from discussions with Baozhi Lin and Yalin Kuo. We are grateful for the constructive reviews provided by Robert Sparkes and an anonymous reviewer. This work is supported by ETH Zurich (ETH-41 14-1) and the National Science Foundation of China (91528304, 41576005, and 41530964).

- Blattmann, T. M., Wessels, M., McIntyre, C. P., & Eglinton, T. I. (2018). Projections for future radiocarbon content in dissolved inorganic carbon in hardwater lakes: A retrospective approach. *Radiocarbon*, *60*(03), 791–800. <https://doi.org/10.1017/RDC.2018.12>
- Bouchez, J., Beyssac, O., Galy, V., Gaillardet, J., France-Lanord, C., Maurice, L., & Moreira-Turcq, P. (2010). Oxidation of petrogenic organic carbon in the Amazon floodplain as a source of atmospheric CO₂. *Geology*, *38*(3), 255–258. <https://doi.org/10.1130/g30608.1>
- Chen, Q., Shen, C., Sun, Y., Peng, S., Yi, W., Li, Z., & Jiang, M. (2008). Soil carbon dynamics in a subtropical mountainous region, South China: Results based on carbon isotopic tracing. In Q. Huang, P. M. Huang, & A. Violante (Eds.), *Soil mineral microbe-organic interactions* (pp. 233–257). New York: Springer.
- Dadson, S., Hovius, N., Pegg, S., Dade, W. B., Horng, M. J., & Chen, H. (2005). Hyperpycnal river flows from an active mountain belt. *Journal of Geophysical Research*, *110*, F04016. <https://doi.org/10.1029/2004JF000244>
- Ding, P., Shen, C., Wang, N., Yi, W., Ding, X., Fu, D., et al. (2010). Turnover rate of soil organic matter and origin of soil ¹⁴C in deep soil from a subtropical forest in Dinghushan Biosphere Reserve, South China. *Radiocarbon*, *52*(03), 1422–1434. <https://doi.org/10.1017/S0033822200046506>
- Ding, P., Shen, C., Wang, N., Yi, W., Ding, X., Fu, D., & Liu, K. (2012). Stratigraphic chronology and sedimentary characteristics for buried ancient forests in the Pearl River Delta. *Quaternary Sciences*, *32*(3), 454–464. <https://doi.org/10.3969/j.issn.1001-7410.2012.03.11>
- Galy, V., Beyssac, O., France-Lanord, C., & Eglinton, T. (2008). Recycling of graphite during Himalayan erosion: A geological stabilization of carbon in the crust. *Science*, *322*(5903), 943–945. <https://doi.org/10.1126/science.1161408>
- Galy, V., Peucker-Ehrenbrink, B., & Eglinton, T. (2015). Global carbon export from the terrestrial biosphere controlled by erosion. *Nature*, *521*(7551), 204–207. <https://doi.org/10.1038/nature14400>
- Gao, Q., Tao, Z., Yao, G., Ding, J., Liu, Z., & Liu, K. (2007). Elemental and isotopic signatures of particulate organic carbon in the Zengjiang River, southern China. *Hydrological Processes*, *21*(10), 1318–1327. <https://doi.org/10.1002/hyp.6358>
- Hedges, J. I. (1992). Global biogeochemical cycles: Progress and problems. *Marine Chemistry*, *39*(1-3), 67–93. [https://doi.org/10.1016/0304-4203\(92\)90096-5](https://doi.org/10.1016/0304-4203(92)90096-5)
- Hedges, J. I., & Stern, J. H. (1984). Carbon and nitrogen determinations of carbonate-containing solids. *Limnology and Oceanography*, *29*(3), 657–663. <https://doi.org/10.4319/lo.1984.29.3.0657>
- Hilton, R. G., Gaillardet, J., Calmels, D., & Birck, J.-L. (2014). Geological respiration of a mountain belt revealed by the trace element rhenium. *Earth and Planetary Science Letters*, *403*, 27–36. <https://doi.org/10.1016/j.epsl.2014.06.021>
- Hilton, R. G., Galy, A., Hovius, N., Chen, M.-C., Horng, M.-J., & Chen, H. (2008). Tropical-cyclone-driven erosion of the terrestrial biosphere from mountains. *Nature Geoscience*, *1*(11), 759–762. <https://doi.org/10.1038/ngeo333>
- Hilton, R. G., Galy, A., Hovius, N., Horng, M.-J., & Chen, H. (2010). The isotopic composition of particulate organic carbon in mountain rivers of Taiwan. *Geochimica et Cosmochimica Acta*, *74*(11), 3164–3181. <https://doi.org/10.1016/j.gca.2010.03.004>
- Hilton, R. G., Galy, A., Hovius, N., Horng, M.-J., & Chen, H. (2011). Efficient transport of fossil organic carbon to the ocean by steep mountain rivers: An orogenic carbon sequestration mechanism. *Geology*, *39*(1), 71–74. <https://doi.org/10.1130/g31352.1>
- Hilton, R. G., Galy, V., Gaillardet, J., Dellinger, M., Bryant, C., O'Regan, M., et al. (2015). Erosion of organic carbon in the Arctic as a geological carbon dioxide sink. *Nature*, *524*(7563), 84–87. <https://doi.org/10.1038/nature14653>
- Hsu, F.-H., Su, C.-C., Wang, C.-H., Lin, S., Liu, J., & Huh, C.-A. (2014). Accumulation of terrestrial organic carbon on an active continental margin offshore southwestern Taiwan: Source-to-sink pathways of river-borne organic particles. *Journal of Asian Earth Sciences*, *91*, 163–173. <https://doi.org/10.1016/j.jseaes.2014.05.006>
- Hwang, J., Druffel, E. R. M., & Eglinton, T. I. (2010). Widespread influence of resuspended sediments on oceanic particulate organic carbon: Insights from radiocarbon and aluminum contents in sinking particles. *Global Biogeochemical Cycles*, *24*, GB4016. <https://doi.org/10.1029/2010GB003802>
- Hwang, J., Eglinton, T. I., Krishfield, R. A., Manganini, S. J., & Honjo, S. (2008). Lateral organic carbon supply to the deep Canada Basin. *Geophysical Research Letters*, *35*, L11607. <https://doi.org/10.1029/2008GL034271>
- Hwang, J., Kim, M., Manganini, S. J., McIntyre, C. P., Haghipour, N., Park, J., et al. (2015). Temporal and spatial variability of particle transport in the deep Arctic Canada Basin. *Journal of Geophysical Research, Oceans*, *120*, 2784–2799. <https://doi.org/10.1002/2014JC010643>
- Hwang, J., Manganini, S. J., Montluçon, D. B., & Eglinton, T. I. (2009). Dynamics of particle export on the Northwest Atlantic margin. *Deep Sea Research Part I: Oceanographic Research Papers*, *56*(10), 1792–1803. <https://doi.org/10.1016/j.dsr.2009.05.007>
- Kao, S., Hilton, R., Selvaraj, K., Dai, M., Zehetner, F., Huang, J., et al. (2014). Preservation of terrestrial organic carbon in marine sediments offshore Taiwan: Mountain building and atmospheric carbon dioxide sequestration. *Earth Surface Dynamics*, *2*(1), 127–139. <https://doi.org/10.5194/esurf-2-127-2014>
- Kao, S.-J., & Liu, K.-K. (1996). Particulate organic carbon export from a subtropical mountainous river (Lanyang Hsi) in Taiwan. *Limnology and Oceanography*, *41*(8), 1749–1757. <https://doi.org/10.4319/lo.1996.41.8.1749>
- Kienast, M., Calvert, S. E., Pelejero, C., & Grimalt, J. O. (2001). A critical review of marine sedimentary $\delta^{13}\text{C}_{\text{org}}$ -pCO₂ estimates: New palaeorecords from the South China Sea and a revisit of other low-latitude $\delta^{13}\text{C}_{\text{org}}$ -pCO₂ records. *Global Biogeochemical Cycles*, *15*(1), 113–127. <https://doi.org/10.1029/2000GB001285>
- Kienast, M., Higginson, M. J., Mollenhauer, G., Eglinton, T. I., Chen, M. T., & Calvert, S. E. (2005). On the sedimentological origin of down-core variations of bulk sedimentary nitrogen isotope ratios. *Paleoceanography*, *20*, PA2009. <https://doi.org/10.1029/2004PA001081>
- Kim, M., Hwang, J., Rho, T., Lee, T., Kang, D.-J., Chang, K.-I., et al. (2017). Biogeochemical properties of sinking particles in the southwestern part of the East Sea (Japan Sea). *Journal of Marine Systems*, *167*, 33–42. <https://doi.org/10.1016/j.jmarsys.2016.11.001>
- Komada, T., Anderson, M. R., & Dorfmeier, C. L. (2008). Carbonate removal from coastal sediments for the determination of organic carbon and its isotopic signatures, $\delta^{13}\text{C}$ and $\Delta^{14}\text{C}$: Comparison of fumigation and direct acidification by hydrochloric acid. *Limnology and Oceanography: Methods*, *6*(6), 254–262. <https://doi.org/10.4319/lom.2008.6.254>
- Komada, T., Druffel, E. R. M., & Trumbore, S. E. (2004). Oceanic export of relict carbon by small mountainous rivers. *Geophysical Research Letters*, *31*, L07504. <https://doi.org/10.1029/2004GL019512>
- Liu, J. T., Wang, Y.-H., Yang, R. J., Hsu, R. T., Kao, S.-J., Lin, H.-L., & Kuo, F. H. (2012). Cyclone-induced hyperpycnal turbidity currents in a submarine canyon. *Journal of Geophysical Research*, *117*, C04033. <https://doi.org/10.1029/2011JC007630>
- Liu, K.-K., Kao, S.-J., Hu, H.-C., Chou, W.-C., Hung, G.-W., & Tseng, C.-M. (2007). Carbon isotopic composition of suspended and sinking particulate organic matter in the northern South China Sea—From production to deposition. *Deep Sea Research Part II: Topical Studies in Oceanography*, *54*(14-15), 1504–1527. <https://doi.org/10.1016/j.dsr2.2007.05.010>
- Liu, Z., Colin, C., Li, X., Zhao, Y., Tuo, S., Chen, Z., et al. (2010). Clay mineral distribution in surface sediments of the northeastern South China Sea and surrounding fluvial drainage basins: Source and transport. *Marine Geology*, *277*(1-4), 48–60. <https://doi.org/10.1016/j.margeo.2010.08.010>

- Liu, Z., Li, X., Colin, C., & Ge, H. (2010). A high-resolution clay mineralogical record in the northern South China Sea since the Last Glacial Maximum, and its time series provenance analysis. *Chinese Science Bulletin*, 55(35), 4058–4068. <https://doi.org/10.1007/s11434-010-4149-5>
- Liu, Z., Zhao, M., Sun, H., Yang, R., Chen, B., Yang, M., et al. (2017). “Old” carbon entering the South China Sea from the carbonate-rich Pearl River Basin: Coupled action of carbonate weathering and aquatic photosynthesis. *Applied Geochemistry*, 78, 96–104. <https://doi.org/10.1016/j.apgeochem.2016.12.014>
- Liu, Z., Zhao, Y., Colin, C., Siringan, F. P., & Wu, Q. (2009). Chemical weathering in Luzon, Philippines from clay mineralogy and major-element geochemistry of river sediments. *Applied Geochemistry*, 24(11), 2195–2205. <https://doi.org/10.1016/j.apgeochem.2009.09.025>
- Liu, Z., Zhao, Y., Colin, C., Stattegger, K., Wiesner, M. G., Huh, C.-A., et al. (2016). Source-to-sink transport processes of fluvial sediments in the South China Sea. *Earth-Science Reviews*, 153, 238–273. <https://doi.org/10.1016/j.earscirev.2015.08.005>
- McIntyre, C. P., Wacker, L., Haghypour, N., Blattmann, T. M., Fahrni, S., Usman, M., et al. (2016). Online ^{13}C and ^{14}C gas measurements by EA-IRMS-AMS at ETH Zürich. *Radiocarbon*, 59(03), 893–903. <https://doi.org/10.1017/RDC.2016.68>
- Meyers, P. A. (1994). Preservation of elemental and isotopic source identification of sedimentary organic matter. *Chemical Geology*, 114(3-4), 289–302. [https://doi.org/10.1016/0009-2541\(94\)90059-0](https://doi.org/10.1016/0009-2541(94)90059-0)
- Sauramo, M. R. (1938). The mode of occurrence of carbon in Quaternary deposits. *Suomen Kemistilehti B*, 3(11), 11–16.
- Sauramo, M. R. (1939). Graphit als Bestandteil der Baltischen Sedimente. *Geologie der Meere und Binnengewässer*, 3, 1–8.
- Schlünz, B., & Schneider, R. R. (2000). Transport of terrestrial organic carbon to the oceans by rivers: Re-estimating flux- and burial rates. *International Journal of Earth Sciences*, 88(4), 599–606. <https://doi.org/10.1007/s005310050290>
- Selvaraj, K., Lee, T. Y., Yang, J. Y. T., Canuel, E. A., Huang, J. C., Dai, M., et al. (2015). Stable isotopic and biomarker evidence of terrigenous organic matter export to the deep sea during tropical storms. *Marine Geology*, 364, 32–42. <https://doi.org/10.1016/j.margeo.2015.03.005>
- Shen, C., Beer, J., Ivy-Ochs, S., Sun, Y., Yi, W., Kubik, P., et al. (2004). ^{10}Be , ^{14}C distribution, and soil production rate in a soil profile of a grassland slope at Heshan Hilly Land, Guangdong. *Radiocarbon*, 46(01), 445–454. <https://doi.org/10.1017/S0033822200039758>
- Shen, C., Sun, Y., Yi, W., Peng, S., & Li, Z. (2001). Carbon isotope tracers for the restoration of degenerated forest ecosystem. *Quaternary Sciences*, 21(5), 452–460.
- Shen, C., Yi, W., Sun, Y., Xing, C., Yang, Y., Yuan, C., et al. (2001). Distribution of ^{14}C and ^{13}C in forest soils of the Dinghushan Biosphere Reserve. *Radiocarbon*, 43(2B), 671–678. <https://doi.org/10.1017/S0033822200041321>
- Shipboard Scientific Party (2000). Site 1144. in Wang, P., Prell, W.L., Blum, P., et al. *Proceedings of the Ocean Drilling Program Initial Reports*, 184(Chapter 5), 1–97. <https://doi.org/10.2973/odp.proc.ir.184.105.2000>
- Sparkes, R. B., Lin, I.-T., Hovius, N., Galy, A., Liu, J. T., Xu, X., & Yang, R. (2015). Redistribution of multi-phase particulate organic carbon in a marine shelf and canyon system during an exceptional river flood: Effects of Typhoon Morakot on the Gaoping River–Canyon system. *Marine Geology*, 363, 191–201. <https://doi.org/10.1016/j.margeo.2015.02.013>
- Talling, P. J., Paull, C. K., & Piper, D. J. W. (2013). How are subaqueous sediment density flows triggered, what is their internal structure and how does it evolve? Direct observations from monitoring of active flows. *Earth-Science Reviews*, 125, 244–287. <https://doi.org/10.1016/j.earscirev.2013.07.005>
- Tao, Z., Gao, Q., Huang, X., Liu, K., Ding, X., & Fu, D. (2012). Biogeochemical cycle of riverine carbon in the Guijiang River: Tracing with ^{14}C and ^{13}C . *Quaternary Sciences*, 32(3), 465–472. <https://doi.org/10.3969/j.issn.1001-7410.2012.03.12>
- Tsai, F., Hwang, J.-H., Chen, L.-C., & Lin, T.-H. (2010). Post-disaster assessment of landslides in southern Taiwan after 2009 Typhoon Morakot using remote sensing and spatial analysis. *Natural Hazards and Earth System Sciences*, 10(10), 2179–2190. <https://doi.org/10.5194/nhess-10-2179-2010>
- Wacker, L., & Christl, M. (2011). Data reduction for small radiocarbon samples: Error propagation using the model of constant contamination. *Ion Beam Physics Annual Report*, 36.
- Wacker, L., Christl, M., & Synal, H. A. (2010). Bats: A new tool for AMS data reduction. *Nuclear Instruments and Methods in Physics Research Section B: Beam Interactions with Materials and Atoms*, 268(7-8), 976–979. <https://doi.org/10.1016/j.nimb.2009.10.078>
- Wacker, L., Fahrni, S. M., Hajdas, I., Molnar, M., Synal, H. A., Szidat, S., & Zhang, Y. L. (2013). A versatile gas interface for routine radiocarbon analysis with a gas ion source. *Nuclear Instruments and Methods in Physics Research Section B: Beam Interactions with Materials and Atoms*, 294, 315–319. <https://doi.org/10.1016/j.nimb.2012.02.009>
- Wang, Y., Fan, D., Liu, J. T., & Chang, Y. (2016). Clay-mineral compositions of sediments in the Gaoping River-Sea system: Implications for weathering, sedimentary routing and carbon cycling. *Chemical Geology*, 447, 11–26. <https://doi.org/10.1016/j.chemgeo.2016.10.024>
- Wei, X., Shen, C., Li, N., Wang, F., Ding, P., Wang, N., et al. (2010). Apparent ages of suspended sediment and soil erosion of the Pearl River (Zhujiang) drainage basin. *Chinese Science Bulletin*, 268(7-8), 1094–1097. <https://doi.org/10.1016/j.nimb.2009.10.107>
- Wei, X., Yi, W., Shen, C., Yechieli, Y., Li, N., Ding, P., et al. (2010). ^{14}C as a tool for evaluating riverine POC sources and erosion of the Zhujiang (Pearl River) drainage basin, South China. *Nuclear Instruments and Methods in Physics Research Section B: Beam Interactions with Materials and Atoms*, 268(7-8), 1094–1097. <https://doi.org/10.1016/j.nimb.2009.10.107>
- Yoneyama, T. (1998). Quantitative analysis of soil organic carbon turnover by using natural abundance of carbon isotopes *Final Reports of Research Projects by The Global Environment Research Fund* (Vol. project B-6.2.3, pp. 285-290).
- Yoneyama, T., Dacanay, E. V., Castelo, O., Kasajima, I., & Ho, P. Y. (2004). Estimation of soil organic carbon turnover using natural ^{13}C abundance in Asian tropics: A case study in the Philippines. *Soil Science & Plant Nutrition*, 50(4), 599–602. <https://doi.org/10.1080/00380768.2004.10408517>
- Yui, T.-F. (2005). Isotopic composition of carbonaceous material in metamorphic rocks from the mountain belt of Taiwan. *International Geology Review*, 47(3), 310–325. <https://doi.org/10.2747/0020-6814.47.3.310>
- Zhang, J., Yi, W., Shen, C., Ding, P., Ding, X., Fu, D., & Liu, K. (2013). Quantification of sedimentary organic carbon storage and turnover of tidal mangrove stands in southern China based on carbon isotopic measurements. *Radiocarbon*, 55(3-4), 1665–1674. https://doi.org/10.2458/azu_js_rc.55.16132
- Zhang, J.-P., Shen, C.-D., Ren, H., Wang, J., & Han, W.-D. (2012). Estimating change in sedimentary organic carbon content during mangrove restoration in southern China using carbon isotopic measurements. *Pedosphere*, 22(1), 58–66. [https://doi.org/10.1016/S1002-0160\(11\)60191-4](https://doi.org/10.1016/S1002-0160(11)60191-4)
- Zhang, Y., Liu, Z., Zhao, Y., Colin, C., Zhang, X., Wang, M., et al. (2018). Long-term in situ observations on typhoon-triggered turbidity currents in the deep sea. *Geology*, 46(8), 675–678. <https://doi.org/10.1130/G45178.1>
- Zhang, Y., Liu, Z., Zhao, Y., Wang, W., Li, J., & Xu, J. (2014). Mesoscale eddies transport deep-sea sediments. *Scientific Reports*, 4(1), 5937. <https://doi.org/10.1038/srep05937>

- Zhao, S., Liu, Z., Chen, Q., Wang, X., Shi, J., Jin, H., et al. (2017). Spatiotemporal variations of deep-sea sediment components and their fluxes since the last glaciation in the northern South China Sea. *Science China Earth Sciences*, *60*(7), 1368–1381. <https://doi.org/10.1007/s11430-016-9058-6>
- Zheng, L.-W., Ding, X., Liu, J. T., Li, D., Lee, T.-Y., Zheng, X., et al. (2017). Isotopic evidence for the influence of typhoons and submarine canyons on the sourcing and transport behavior of biospheric organic carbon to the deep sea. *Earth and Planetary Science Letters*, *465*, 103–111. <https://doi.org/10.1016/j.epsl.2017.02.037>
- Zhou, B., Bird, M., Zheng, H., Zhang, E., Wurster, C. M., Xie, L., & Taylor, D. (2017). New sedimentary evidence reveals a unique history of C4 biomass in continental East Asia since the early Miocene. *Scientific Reports*, *7*(1), 170. <https://doi.org/10.1038/s41598-017-00285-7>